J Mater Sci (2009) 44:5375–5382
DOI 10.1007/s10853-009-3569-6

FERROELECTRICS

Heterolayered PZT thin films of different thicknesses and stacking sequence

F. C. Kartawidjaja · C. H. Sim · J. Wang

Received: 25 March 2009 / Accepted: 12 May 2009 / Published online: 30 May 2009
© Springer Science+Business Media, LLC 2009

Abstract The effects of stacking sequence and thickness toward the texture and electrical properties of heterolayered $PbZr_xTi_{1-x}O_3$ (PZT) films, consisting of alternating $PbZr_{0.7}Ti_{0.3}O_3$ and $PbZr_{0.3}Ti_{0.7}O_3$ layers, have been studied. Thickness dependence is observed in the ferroelectric and dielectric behavior of the heterolayered PZT films whereby the remanent polarization (P_r) and relative permittivity (ε) increase with thickness, while coercive field (E_c) decreases. When baked at 500 °C and thermally annealed at 650 °C, the heterolayered PZT films regardless of their stacking sequence exhibit perovskite phase with (001)/(100) preferred orientation. Interestingly, the stacking sequence of the heterolayered PZT films dictates the morphology of the films which eventually affects the ferroelectric and dielectric performance. The heterolayered PZT film with $PbZr_{0.7}Ti_{0.3}O_3$ as the first layer (heterolayered $PZ_{70}T_{30}$ film) exhibits a large grain size in the range of 1–3 μm and shows superior properties as compared to the heterolayered PZT films with $PbZr_{0.3}Ti_{0.7}O_3$ as the first layer (heterolayered $PZ_{30}T_{70}$ film), which exhibits a much smaller grain size. From the sub-switching field measurement according to the Rayleigh law, there appears a lower concentration or mobility of domain walls in the small-grained heterolayered $PZ_{30}T_{70}$ films.

F. C. Kartawidjaja · C. H. Sim · J. Wang (✉)
Department of Materials Science & Engineering, Faculty of Engineering, National University of Singapore, Singapore 117574, Singapore
e-mail: msewangj@nus.edu.sg

Introduction

There have been intensive on-going investigations into novel ferroelectric thin films, in attempts to find better materials or to improve the electrical properties of the existing ferroelectric thin films via novel processing routes, motivated by the expectation that they revolutionize the performance of various devices such as sensors, actuators, NVRAM, and MEMs [1–5]. Recently, the research on multilayered ferroelectric structures, which are formed by stacking different ferroelectric materials, such as epitaxial $PbTiO_3/PbZrO_3$ [6] and $BaTiO_3/SrTiO_3$ [7, 8] films or by stacking compositionally graded layers such as $(Pb_y,Ca_{1-y})TiO_3$ [9] and $Pb_{1-3y/2}La_y(Zr_{0.4}Ti_{0.6})O$ [10], has been carried out extensively. It has been reported that these multilayered structures exhibit outstanding electrical properties which are much better than those of its single ferroelectric constituent or they can effectively combine the desired properties of the ferroelectric layers. For example, $(Bi,La)_4Ti_3O_{12}/Pb(Zr_{0.4}Ti_{0.6})O_3/(Bi,La)_4Ti_3O_{12}$ trilayered thin film is reported to exhibit a high fatigue resistance up to 10^{10} switching pulse accompanied with excellent ferroelectric properties [11]. Zhong et al. [12] reported that the compositionally graded multilayered BST film shows a high tunability over a wide range of temperature. The effect of sequence in multilayered thin films has also been brought to attention by several researchers whereby they observed that desirable properties could be obtained by tailoring the sequence of the constituent layers in the multilayered structure [13, 14].

More recently, investigations have been made into heterolayered $PbZr_xTi_{1-x}O_3$ (PZT) thin films, whereby much improved ferroelectric and dielectric properties have been demonstrated [15–18]. For example, Zhou et al. [18] reported on a giant P_r value of 71.9 μC/cm^2 and a relative

permittivity of 905 for heterolayered PZT films consisting of alternating $PbZr_{0.8}Ti_{0.2}O_3$ and $PbZr_{0.2}Ti_{0.8}O_3$ layers with $PbZr_{0.8}Ti_{0.2}O_3$ as the first layer. We have also reported that the heterolayered PZT film consisting of alternating $PbZr_{0.7}Ti_{0.}O_3$ and $PbZr_{0.3}Ti_{0.7}O_3$ layers with $PbZr_{0.7}Ti_{0.3}O_3$ as the first layer shows much improved ferroelectric and dielectric properties as compared to the $PbZr_{0.7}Ti_{0.}O_3$ and $PbZr_{0.3}Ti_{0.7}O_3$ thin films [15].

PZT was chosen for study because it has long been known for its excellent dielectric, large spontaneous polarization, and desired piezoelectric behavior [19, 20]. However, it is also associated with a couple of limitations when fabricated into thin film forms. Among others, it has been reported that the ferroelectric and dielectric properties of PZT film degrade with decreasing thickness [21–23]. This phenomenon is observed especially when Pt is used as the electrode. The interface space charge layer, formed as a result of the interaction between the dielectric film and the top/bottom electrodes, plays a dominant role as the thickness of the film decreases to below 100 nm resulting in a reduction in the relative permittivity of the capacitor structure. This study is aimed at fully understanding the ferroelectric and dielectric behavior of the heterolayered PZT films consisting of alternating $PbZr_{0.7}Ti_{0.}O_3$ and $PbZr_{0.3}Ti_{0.7}O_3$ layers, as a function of thickness and different stacking sequence of the heterolayered structure.

Experimental details

The heterolayered PZT films were deposited through a multi-step sol–gel processing route, by spin coating the $Pb(Zr_{0.7}Ti_{0.3})O_3$ and $Pb(Zr_{0.3}Ti_{0.7})O_3$ precursor solutions with 10 mol% excess lead and concentration of 0.4 M. To fabricate the heterolayered $PZ_{70}T_{30}$ film, the $Pb(Zr_{0.7}Ti_{0.3})O_3$ precursor solution was first made and spin-coated onto the $Pt/Ti/SiO_2/Si$ substrate at 3000 rpm for 30 s, followed by drying and thermal baking at 300 and 500 °C, respectively. The $Pb(Zr_{0.3}Ti_{0.7})O_3$ precursor solution was then prepared and spin-coated as the second layer by following the same procedure. The stacking sequence was switched for the heterolayered $PZ_{30}T_{70}$ thin films, which means that $Pb(Zr_{0.3}Ti_{0.7})O_3$ was spin-coated as the first layer followed by $Pb(Zr_{0.7}Ti_{0.3})O_3$ as the second layer. These procedures were repeated several times until the desired number of layers was obtained, before it was finally annealed for 1.0 h at 650 °C in a RTP chamber. Heterolayered $PZ_{70}T_{30}$ and heterolayered $PZ_{30}T_{70}$ films consisting of two (coded as 2-heterolayer, thickness ~150 nm) and six layers (coded as 6-heterolayer, thickness ~450 nm) were deposited for investigation, as illustrated in Fig. 1.

X-ray diffraction (XRD) was employed to study the phases present in and crystallinities of the heterolayered films. The surface morphologies were characterized using Atomic Force Microscopy (AFM). Solartron impedance analyzer and Radiant Precise Workstation were employed to study their dielectric and ferroelectric behavior, respectively. The compositional depth profiling of the heterolayered PZT thin films was investigated by using secondary ion mass spectroscopy (SIMS).

Results and discussion

The XRD traces of the heterolayered $PZ_{70}T_{30}$ and $PZ_{30}T_{70}$ thin films after thermal annealing at 650 °C are shown in Fig. 2. The respective phases of $PZ_{70}T_{30}$ and $PZ_{30}T_{70}$ layers are well-retained in the heterolayered films and they are fully crystallized into perovskite, as the pyrochlore phase identifiable at 29.5° is not observed in the XRD traces. It is of interest to note that the heterolayered films show the high intensity of (001)/(100) peaks, regardless of the stacking sequence. It has been reported that at a baking temperature of 500 °C, $PZ_{30}T_{70}$ layer was crystallized into perovskite phase with the (100) orientation [24, 25]. It is suggested that in the heterolayered configuration, the $PZ_{30}T_{70}$ layer dictates the crystallization and orientation of $PZ_{70}T_{30}$ layer which exhibits a higher crystallization

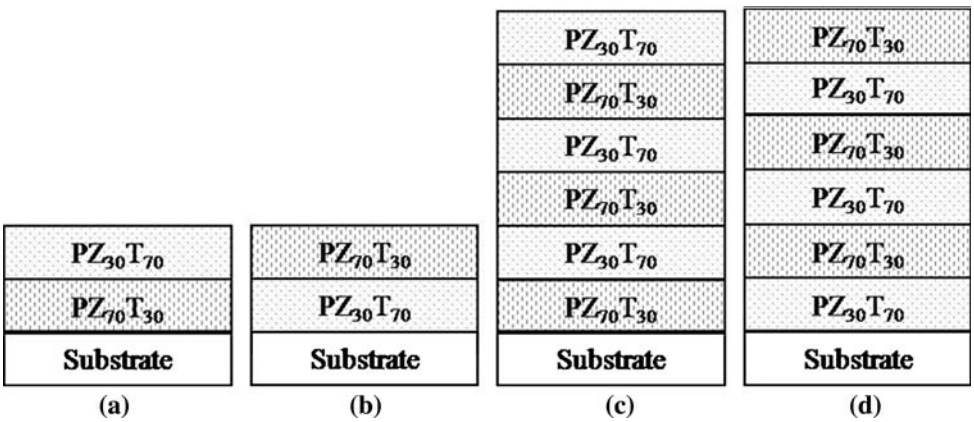

Fig. 1 Schematic diagrams of **a** $PZ_{70}T_{30}$ 2-heterolayer, **b** $PZ_{30}T_{70}$ 2-heterolayer, **c** $PZ_{70}T_{30}$ 6-heterolayer, and **d** $PZ_{30}T_{70}$ 6-heterolayer thin films

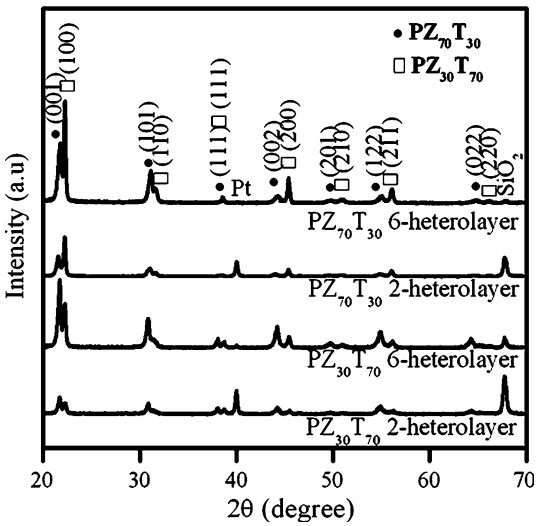

Fig. 2 XRD traces of the heterolayered $PZ_{70}T_{30}$ and heterolayered $PZ_{30}T_{70}$ thin films after thermal annealing at 650 °C for 1 h

temperature. This resulted in the (001)/(100) preferred orientation of heterolayered PZT films when baked at 500 °C, regardless of the stacking sequence.

The preservation of the $PZ_{70}T_{30}$ and $PZ_{30}T_{70}$ layers in the heterolayered PZT films is further confirmed by the SIMS profiles for $PZ_{70}T_{30}$ 6-heterolayer and $PZ_{30}T_{70}$ 6-heterolayer, as shown in Fig. 3a and b, respectively. The regions with higher Zr intensity correspond to $PZ_{70}T_{30}$ layers and regions with higher Ti intensity correspond to $PZ_{30}T_{70}$ layers. The coexistence of the alternating $PZ_{70}T_{30}$ and $PZ_{30}T_{70}$ layers in the heterolayered thin films are indicated by the well-defined boundaries between Zr and Ti elements from Zr-rich layer of $PZ_{70}T_{30}$ and Ti-rich layer of $PZ_{30}T_{70}$. From the SIMS traces, it is also observed that there is a notable degree of inter-diffusion at the interface of the first and second layers as compared to the sharp interface between the subsequent layers in both heterolayered PZT films. The observed SIMS profiling is due to the surface roughness effect. Based on surface roughness measurement by AFM, the first layer is found to exhibit a rougher surface as compared to other layers, which causes the observed gradual change in Zr and Ti intensities from the first to second layer. Increasing the number of layers deposited leads to a film with smooth interface, which gives a sharp SIMS interfacial profiling.

Concerning the film texture studied by using AFM, a comparison of the surface morphology between the heterolayered $PZ_{70}T_{30}$ and heterolayered $PZ_{30}T_{70}$ thin films is presented in Fig. 4. They both show a rather compact and dense film texture and microstructure. Both $PZ_{70}T_{30}$ 2-heterolayer and $PZ_{70}T_{30}$ 6-heterolayer are observed to have unusually large grain size, in the range of 1–3 μm. However, in comparison to the heterolayered $PZ_{70}T_{30}$ film,

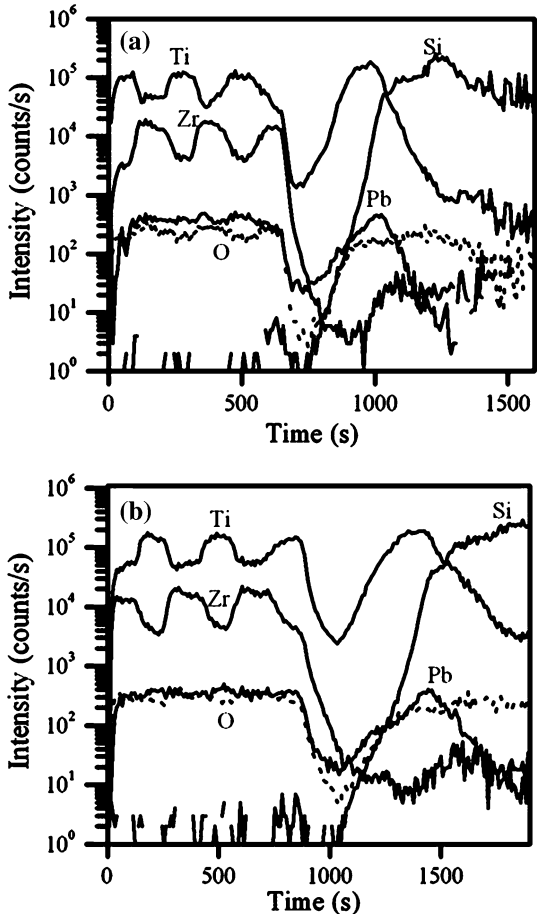

Fig. 3 SIMS compositional depth profiling of **a** $PZ_{70}T_{30}$ 6-heterolayer and **b** $PZ_{30}T_{70}$ 6-heterolayer

the heterolayered $PZ_{30}T_{70}$ thin films show much refined grain size in the range of 80–250 nm. By changing the stacking sequence of the layers, the film texture is changed significantly. The first layer deposited, which acts as a seeding layer, has an important role in dictating the overall film texture of the heterolayered PZT thin films. In the heterolayered $PZ_{30}T_{70}$ films, the top $PZ_{70}T_{30}$ layer follows the texture of the $PZ_{30}T_{70}$ seeding layer which has a smaller grain size as compared to $PZ_{70}T_{30}$. This results in the overall small-grained microstructure as observed in the heterolayered $PZ_{30}T_{70}$ thin films. The refinement in grain size for the heterolayered $PZ_{30}T_{70}$ films leads to a smoother surface as the $PZ_{30}T_{70}$ layer beneath $PZ_{70}T_{30}$ layer reduces the surface roughness of the heterolayered PZT film. For example, the surface roughness of $PZ_{30}T_{70}$ 6-heterolayer is almost 45% lower than that of $PZ_{70}T_{30}$ 6-heterolayer film. The heterolayered PZT film surfaces also smoothen with the increasing number of layers deposited. For example, the surface roughness of heterolayered $PZ_{70}T_{30}$ films decreases from 3.841 to 2.453 nm, when the number of layers is increased from two to six layers, while for the heterolayered $PZ_{30}T_{70}$ films, it changes from 2.649 to 1.071 nm.

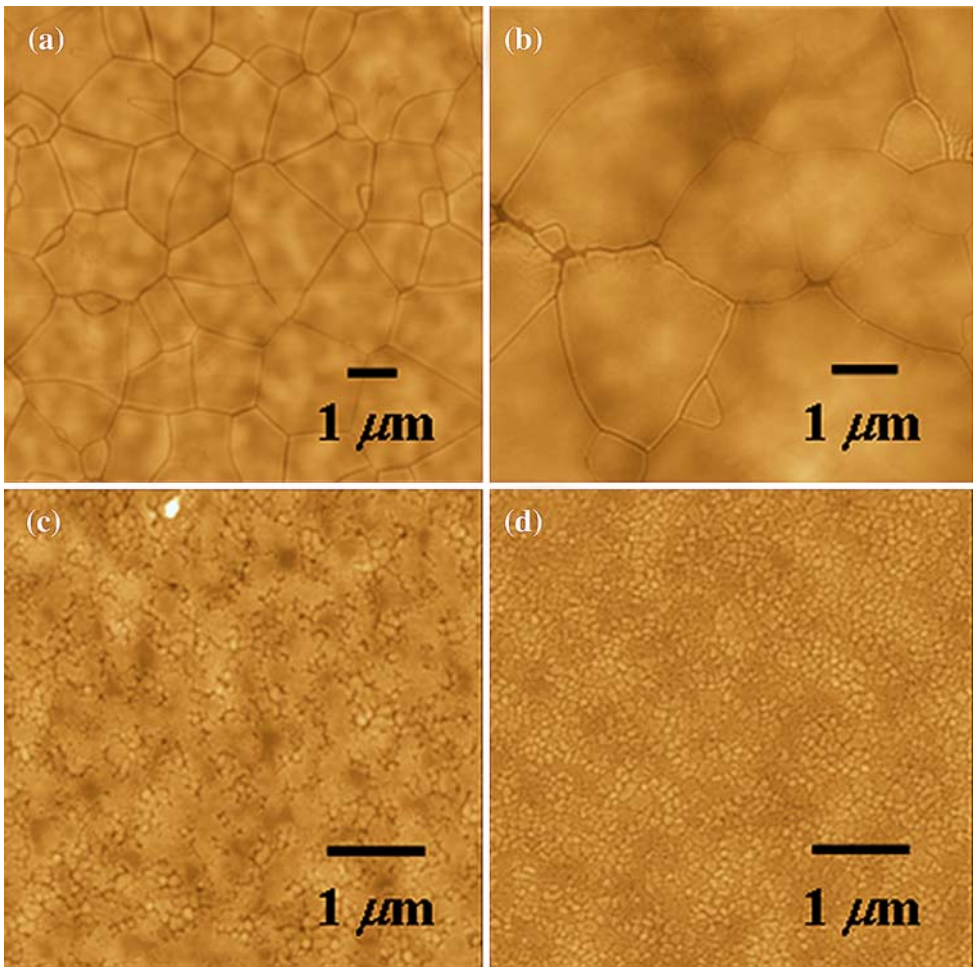

Fig. 4 AFM images showing the surface morphology of **a** $PZ_{70}T_{30}$ 2-heterolayer, **b** $PZ_{70}T_{30}$ 6-heterolayer, **c** $PZ_{30}T_{70}$ 2-heterolayer, and **d** $PZ_{30}T_{70}$ 6-heterolayer thin films

Figure 5 shows the hysteresis loops of the heterolayered PZT films measured with increasing electric field from 300 to 1000 kV/cm. It is observed that with increasing thickness, P_r increases while the E_c decreases. For example, the $PZ_{70}T_{30}$ 2-heterolayer film exhibits a P_r value of 19.4 μC/cm^2 and a E_c value of 249 kV/cm, while the $PZ_{70}T_{30}$ 6-heterolayer film exhibits a P_r value of 41.3 μC/cm^2 and a E_c value of 131 kV/cm at an electric field of 1000 kV/cm. Similar observation is noted with the heterolayered $PZ_{30}T_{70}$ films whereby the P_r increases from 15.3 to 24.2 μC/cm^2 and E_c decreases from 163 to 74 kV/cm with increasing thickness. The thickness dependence of coercive field in ferroelectric films has been commonly observed. The explanation behind this phenomenon is attributed to the drop in voltage across the space charge depletion layer which exists at the interface between the ferroelectric film surface and the electrodes [26–28]. The open hysteresis loops observed in Fig. 5 is suggested to be due to the incomplete domain back-switching related with slow domain wall movement as it is pinned by defects [29]. A more interesting observation is noted when one compares the ferroelectric properties between heterolayered $PZ_{70}T_{30}$ and heterolayered $PZ_{30}T_{70}$ films. By changing the stacking sequence of the heterolayered PZT films, the ferroelectric properties are affected greatly. Indeed, the P_r and E_c values of $PZ_{70}T_{30}$ 6-heterolayer are almost double of those of $PZ_{30}T_{70}$ 6-heterolayer film.

The dielectric behavior of the heterolayered PZT films were studied for the relative permittivity (ε) and dielectric loss (tan δ) as a function of frequency (100 Hz–300 kHz) under an applied *ac* field of 0.1 V amplitude, as shown in Fig. 6. Similar to the ferroelectric behavior, there is a thickness dependence of relative permittivity for both the heterolayered $PZ_{70}T_{30}$ and heterolayered $PZ_{30}T_{70}$ thin films. At a frequency of 1 kHz, the relative permittivity increases from 325 to 710 for heterolayered $PZ_{70}T_{30}$ and from 221 to 602 for heterolayered $PZ_{30}T_{70}$ when the number of layers increases from two to six layers. The thickness dependence of the relative permittivity in heterolayered $PZ_{70}T_{30}$ thin films has been suggested to be due to the presence of low-ε interfacial layer between the top/bottom electrodes with the ferroelectric PZT films [30]. To investigate the influence of electrode/film interfacial layers toward the relative permittivity of heterolayered $PZ_{30}T_{70}$ films, the capacitance series connection can be applied [31–33]. Two scenarios are considered in this study. In the first scenario, no electrode/film interface layer is assumed

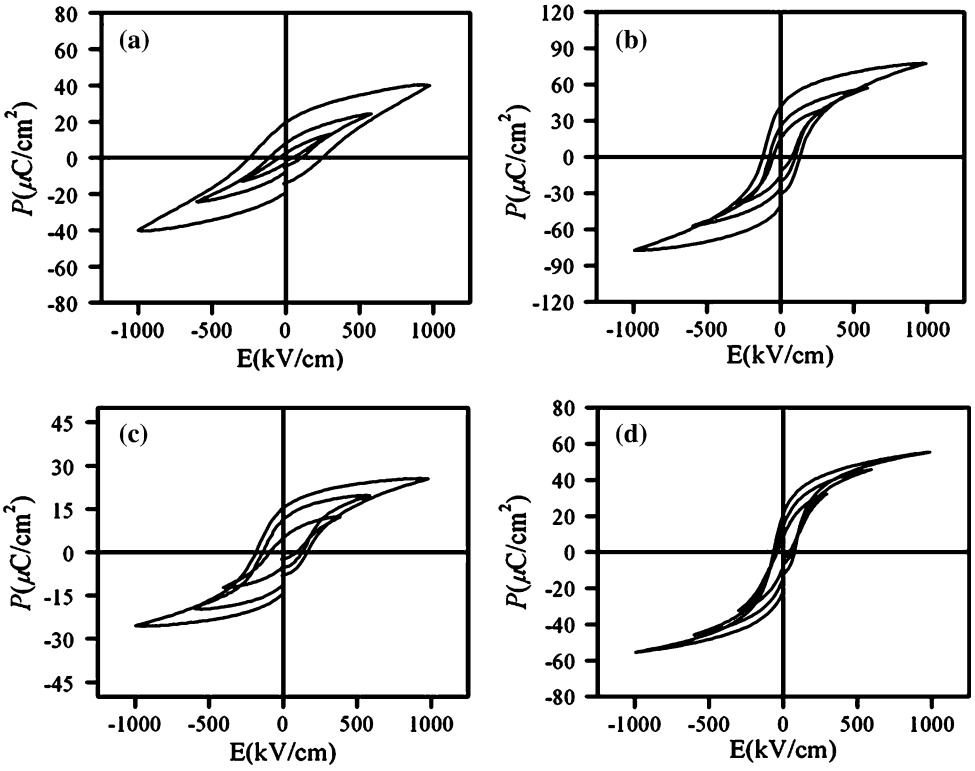

Fig. 5 Hysteresis loops of **a** $PZ_{70}T_{30}$ 2-heterolayer, **b** $PZ_{70}T_{30}$ 6-heterolayer, **c** $PZ_{30}T_{70}$ 2-heterolayer, and **d** $PZ_{30}T_{70}$ 6-heterolayer thin films, respectively

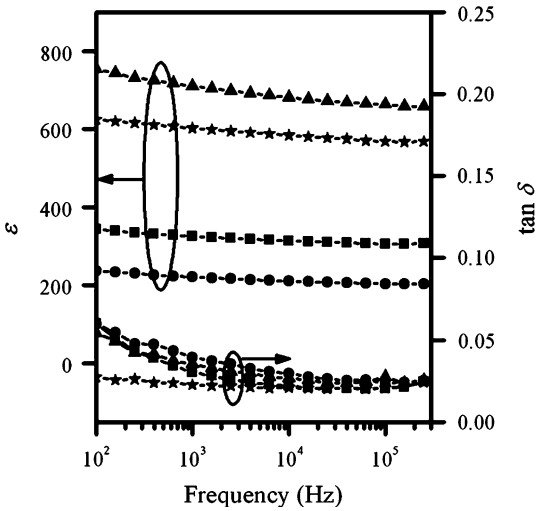

Fig. 6 Dielectric behavior of heterolayered $PZ_{70}T_{30}$ and heterolayered $PZ_{30}T_{70}$thin films. (*filled square*) $PZ_{70}T_{30}$ 2-heterolayer and (*filled triangle*) $PZ_{70}T_{30}$ 6-heterolayer, (*filled circle*) $PZ_{30}T_{70}$ 2-heterolayer and (*filled star*) $PZ_{30}T_{70}$ 6-heterolayer

and the capacitance is thus contributed only from the ferroelectric $PZ_{70}T_{30}$ and $PZ_{30}T_{70}$ layers which can be described with the following equation

$$\frac{1}{C}=\frac{d_t}{\varepsilon_0 A\varepsilon_f}=\frac{1}{\varepsilon_0 A}\left(\frac{d_{PZ_{70}T_{30}}}{\varepsilon_{PZ_{70}T_{30}}}+\frac{d_{PZ_{30}T_{70}}}{\varepsilon_{PZ_{30}T_{70}}}\right), \quad (1)$$

where C is the theoretical capacitance of the film, d and ε are the thickness and relative permittivity of the ferroelectric layer, respectively. In the second scenario, the electrode/film interface layer is considered and the capacitance of the ferroelectric PZT films, and the interfacial layers are considered to be connected in series and is given with the following relationship:

$$\frac{1}{C}=\frac{1}{\varepsilon_0 A}\left(\frac{d_f}{\varepsilon_f}+\frac{d_i}{\varepsilon_i}\right), \quad (2)$$

where d_f and d_i are the thickness of the ferroelectric and interfacial layers, respectively, ε_f and ε_i are the relative permittivity of the ferroelectric and interfacial layer, respectively. In our heterolayered structure, Eq. 2 can be elaborated as the following:

$$\frac{1}{C}=\frac{d_t}{\varepsilon_0 A\varepsilon_f}=\frac{1}{\varepsilon_0 A}\left(\frac{d_{i,Pt/PZ_{30}T_{70}}}{\varepsilon_{i,Pt/PZ_{30}T_{70}}}+\frac{d_{PZ_{70}T_{30}}}{\varepsilon_{PZ_{70}T_{30}}}+\frac{d_{PZ_{30}T_{70}}}{\varepsilon_{PZ_{30}T_{70}}}+\frac{d_{i,PZ_{70}T_{30}/Au}}{\varepsilon_{i,PZ_{70}T_{30}/Au}}\right) \quad (3)$$

Based on our previous study, the relative permittivity of $PZ_{70}T_{30}$ and $PZ_{30}T_{70}$ films are calculated to be 705 and 662, respectively, by plotting the reciprocal of the film capacitance as a function of the film thickness [30]. The total value of $\frac{d_{i,Pt/PZ_{30}T_{70}}}{\varepsilon_{i,Pt/PZ_{30}T_{70}}}$ and $\frac{d_{i,PZ_{70}T_{30}/Au}}{\varepsilon_{i,PZ_{70}T_{30}/Au}}$ is calculated to be 0.1876. The comparison of the relative permittivity for the heterolayered $PZ_{30}T_{70}$ films between the experimental and predicated values are shown in Fig. 7. It is observed that with increasing thickness, the relative permittivity of the

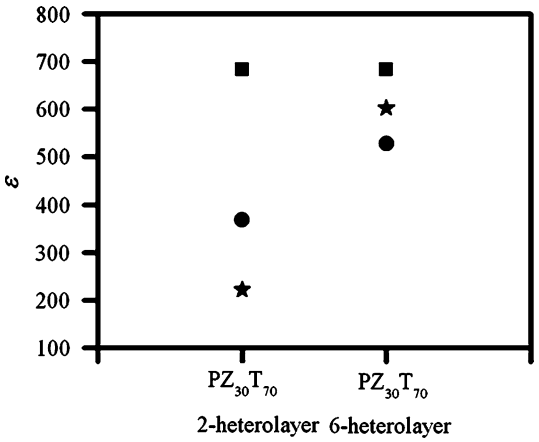

Fig. 7 Comparison of the theoretical values calculated from scenario 1 and 2 with experimental results for the heterolayered $PZ_{30}T_{70}$ thin films. (*filled square*) Theoretical values based on scenario 1, (*filled circle*) theoretical values based on scenario 2, and (*filled star*) experimental values

heterolayered $PZ_{30}T_{70}$ film is closer to the theoretical value of scenario 1 where no electrode/film interfacial layer is considered. The electrode/film interfacial layer is suggested to be the cause of the thickness dependence in the heterolayered $PZ_{30}T_{70}$ thin films. Comparing the heterolayered $PZ_{70}T_{30}$ films with heterolayered $PZ_{30}T_{70}$ films, it is also observed that heterolayered $PZ_{70}T_{30}$ films exhibit higher relative permittivities than those of the heterolayered $PZ_{30}T_{70}$ films with similar thickness.

Further studies at sub-switching field by implementing the Rayleigh law provide useful information on the respective contributions of intrinsic lattice and domain walls movement toward the relative permittivity at sub-switching field. The Rayleigh law is given as the following equation:

$$\varepsilon = \varepsilon_{\text{init}} + \alpha E, \tag{4}$$

whereby $\varepsilon_{\text{init}}$ relates to the reversible contribution and α relates to the irreversible contribution toward the relative permittivity of the films [34, 35]. By looking at the Rayleigh coefficient α, one can obtain useful information on the domain walls mobility or the number of mobile domain walls present in the heterolayered PZT films [36]. Figure 8 shows the relative permittivity of the heterolayered PZT films as a function of applied *ac* field (0–30 kV/cm) at different frequencies (10–10^5 Hz). It gives a linear relationship that follows the Rayleigh law as equated in Eq. 3. The values of $\varepsilon_{\text{init}}$ and α of the film can then be determined from the *y*-intercept and gradient of the linear fit, respectively. The values of α and $\alpha/\varepsilon_{\text{init}}$ at 1 kHz for each of the heterolayered PZT films are plotted in Fig. 9. Comparing the values of α of the heterolayered PZT films, one can observe that there is a film thickness dependence of α, where α increases with increasing number of layers. The

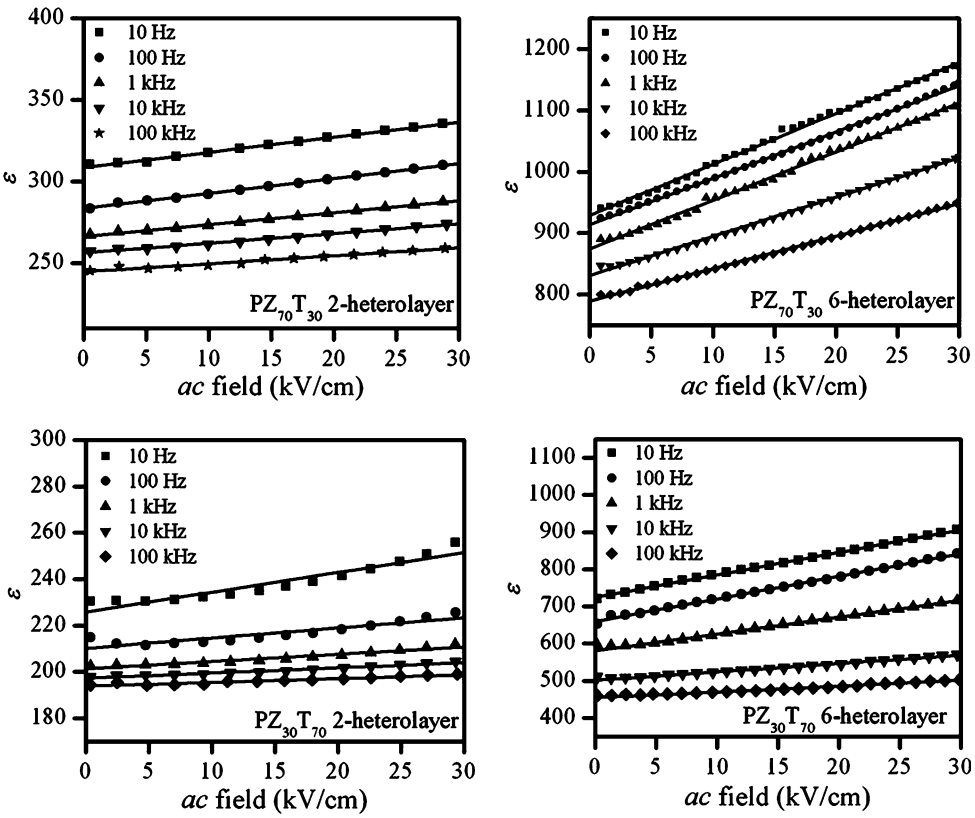

Fig. 8 Field dependence of the relative permittivity for the heterolayered $PZ_{70}T_{30}$ and $PZ_{30}T_{70}$ films at frequencies of 10–100 kHz

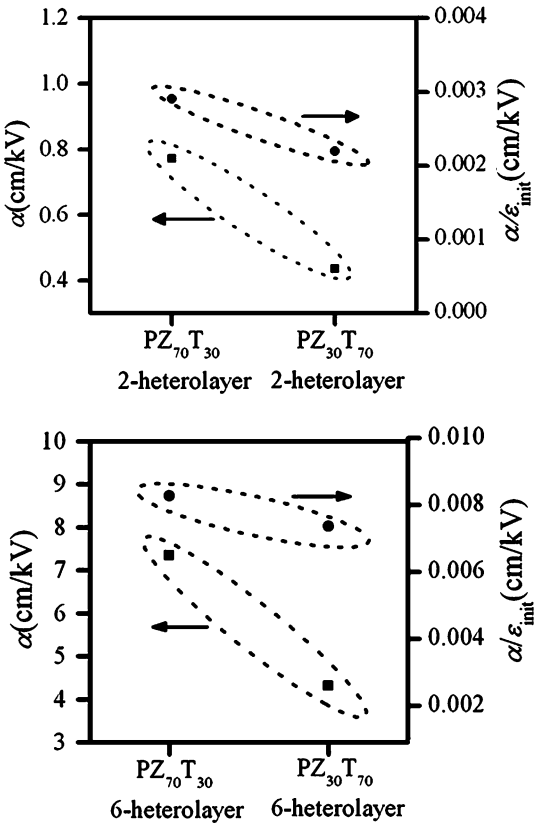

Fig. 9 The irreversible parameter (α) and ratio of the irreversible to the reversible Rayleigh coefficient ($\alpha/\varepsilon_{init}$) for the heterolayered PZT thin films at 1 kHz according to the Rayleigh law

value of α for $PZ_{70}T_{30}$ 2-heterolayer is observed to be 0.77, while the value of α for $PZ_{70}T_{30}$ 6-heterolayer is 7.35 at frequency of 1 kHz. This observation suggests that there is higher mobility of domain walls or in other words, a lower degree of domain wall pinning with increasing layer thickness. Comparing the heterolayered $PZ_{30}T_{70}$ films with the heterolayered $PZ_{70}T_{30}$ films, it is also noted that the heterolayered $PZ_{30}T_{70}$ films exhibit smaller α values than those of heterolayered $PZ_{70}T_{30}$ films. At the frequency of 1 kHz, the α value of $PZ_{70}T_{30}$ 6-heterolayer is 1.5× of the α value of $PZ_{30}T_{70}$ 6-heterolayer. This suggests that there is a fewer number of mobile domain walls or a lower degree of or mobility present in heterolayered $PZ_{30}T_{70}$ relative to the heterolayered $PZ_{70}T_{30}$ thin films. This is further supported by the ratio of the irreversible to the reversible Rayleigh coefficient ($\alpha/\varepsilon_{init}$), where it is observed that the $\alpha/\varepsilon_{init}$ ratio for heterolayered $PZ_{30}T_{70}$ is also lower than that of heterolayered $PZ_{70}T_{30}$ thin film.

Based on the observation presented above, the heterolayered $PZ_{30}T_{70}$ film shows inferior electrical behavior when compared to the heterolayered $PZ_{70}T_{30}$ thin film. As all films undergo the same heating treatment and they show the perovskite phase with (001)/(100) preferred orientation, the differences in dielectric and ferroelectric behavior are attributed to the significant difference in grain sizes between the two films. The average grain size of $PZ_{70}T_{30}$ 6-heterolayer film is indeed 12× larger than that of $PZ_{30}T_{70}$ 6-heterolayer film. There are previous reports that the grain size can strongly affect the physical behavior of ferroelectric films, whereby the ferroelectric and dielectric properties are improved with increasing grain size [37–40]. According to Arlt et al. [41], a decrease in grain size correlates to an increase in the number (density) of ferroelectric 90° domains as the domain width is proportional to the square root of grain size which can be equated as follows:

$$N_d \sim \frac{1}{w} \sim \frac{1}{\sqrt{a}}, \tag{5}$$

where N_d is domain density, w is the domain width, and a is the grain size. On the basis of this correlation, the contribution of 90° domain toward the relative permittivity increases with decreasing grain size, and thus an increase of relative permittivity should be observed as the grain size becomes smaller. However, the repulsive force between the neighboring domain walls also becomes more important as the number of domains increases with decreasing grain size [37]. It restricts the movement of the domain walls which leads to a decrease in relative permittivity and P_r, as observed in the heterolayered $PZ_{30}T_{70}$ thin film. This phenomenon is supported by the observation made with the sub-switching field measurement discussed previously, which shows that the heterolayered $PZ_{30}T_{70}$ thin films exhibit smaller values of α and $\alpha/\varepsilon_{init}$ as compared to the heterolayered $PZ_{70}T_{30}$ thin films due to the lower concentration or mobility of domain walls that attributed to the small grain size of these films. There is a higher mobility of domains in the large-grained heterolayered $PZ_{70}T_{30}$ thin film as the large grains facilitate the movement of domains enhancing the ferroelectric and dielectric behavior.

Conclusions

Heterolayered PZT films, fabricated by sol–gel route, have been investigated for their thickness and stacking sequence dependences of the film texture and electrical behavior. When baked at 500 °C, the $PZ_{30}T_{70}$ layer was crystallized with (100) orientation, which then affected the crystallization and orientation of $PZ_{70}T_{30}$ layer such that the heterolayered PZT films exhibit a (001)/(100) preferred orientation, regardless of their stacking sequence. Significant differences due to the difference in stacking sequence are observed with the heterolayered $PZ_{70}T_{30}$ and heterolayered $PZ_{30}T_{70}$ films in both film texture and electrical behavior. Heterolayered $PZ_{70}T_{30}$ films are observed to exhibit a large-grained texture, 12× larger in size than the

heterolayered $PZ_{30}T_{70}$ thin film. The refined grain microstructure in the heterolayered $PZ_{30}T_{70}$ films causes restriction in the domain mobility as supported by the observation from sub-switching measurement, whereby the heterolayered $PZ_{30}T_{70}$ films show lower Rayleigh constants (α) than those of heterolayered $PZ_{70}T_{30}$ films. The overall film texture plays a key role in determining the electrical properties of the heterolayered PZT films of different stacking sequence. The thickness dependence of ferroelectric and dielectric behavior in heterolayered PZT films can be correlated to the presence of low-ε film/electrode interfacial layers as revealed by the capacitance series connection model.

Acknowledgements This paper is based on work supported by the Science and Engineering Research Council—A*Star, Singapore under Grant No. 012 101 0130. The authors would like to thank Dr. Debbie Seng Hwee Leng for her time and efforts on SIMS measurements and Dr. X.J. Lou for his time in discussion. The authors would like to acknowledge the support of National University of Singapore in this project.

References

1. Scott JF (2000) Ferroelectric memories. Springer, New York
2. Scott JF, Araujo A (1989) Science 246:1400
3. Lee HN, Christen HM, Chisholm MF, Rouleau CM, Lowndes DH (2005) Nature 433:395
4. Cole MW, Ngo E, Hirsch S, Okatan MB, Alpay SP (2008) Appl Phys Lett 92:072906
5. Qin WF, Xiong J, Zhu J, Tang JL, Jie WJ, Zhang Y, Li YR (2008) J Mater Sci 43:409. doi:10.1007/s10853-007-2177-6
6. Kanno I, Hayashi S, Takayama R, Hirao T (1996) Appl Phys Lett 68:328
7. Kim L, Jung D, Kim J, Kim YS, Lee J (2003) Appl Phys Lett 82:2118
8. Shimuta T, Nakagawara O, Makino T, Arai S, Tabata H, Kawai T (2002) J Appl Phys 91:2290
9. Bao D, Zhang L, Yao X (2000) Appl Phys Lett 76:1063
10. Boerasu I, Pintilie L, Kosec M (2000) Appl Phys Lett 77:2231
11. Bao D, Lee SK, Zhu X, Alexe M, Hesse D (2005) Appl Phys Lett 86:082906
12. Zhong S, Alpay SP, Cole MW, Ngo E, Hirsch S, Demaree JD (2007) Appl Phys Lett 90:092901
13. Lee SJ, Moon SE, Ryu HC, Kwak MH, Kim YT, Han SK (2003) Appl Phys Lett 82:2133
14. Sigman J, Clem PG, Nordquist CD (2006) Appl Phys Lett 89:132909
15. Kartawidjaja FC, Zhou ZH, Wang J (2006) J Electroceram 16:425
16. Lee SG, Park IG, Bae SG, Lee YH (1997) Jpn J Appl Phys 36:6880
17. Wu JG, Xiao DQ, Zhu JG, Zhu JL, Tan JZ, Zhang QL (2007) Appl Phys Lett 90:082902
18. Zhou ZH, Xue JM, Li WZ, Wang J, Zhu H, Miao JM (2004) J Appl Phys 96:5706
19. Shi D (2003) Functional thin films and functional materials: new concept and technologies. Springer, New York
20. Bell AJ (2006) J Mater Sci 41:13. doi:10.1007/s10853-005-5913-9
21. Bouregba R, Poullain GLRG, Leclerc G (2006) J Appl Phys 99:034102
22. Cillessen JFM, Prins MWJ, Wolf RM (1997) J Appl Phys 81:2777
23. Mihara T, Yoshimuri H, Watanabe H, Araujo CA (1995) Jpn J Appl Phys 34:5233
24. Chen SY, Chen IW (1998) J Am Ceram Soc 81:97
25. Reaney IM, Brooks KG, Klissurska R, Pawlaczyk C, Setter N (1994) J Am Ceram Soc 77:1209
26. Kanzig W (1955) Phys Rev 98:549
27. Sidorkin AS, Nesterenko LP, Bocharova IA, Sidorkin VA, Smirnov GL (2003) Ferroelectrics 286:335
28. Zubko P, Jung DJ, Scott JF (2006) J Appl Phys 100:114112
29. Zhou ZH, Xue JM, Li WZ, Wang J, Zhu H, Miao JM (2004) Appl Phys Lett 85:804
30. Kartawidjaja FC, Sim CH, Wang J (2007) J Appl Phys 102:124102
31. Ellerkmann U, Liedtke R, Waser R (2002) Ferroelectrics 271:315
32. Lee JJ, Thio CL, Desu SB (1995) J Appl Phys 78:5073
33. Pintilie L, Vrejoiu I, Hesse D, LeRhun G, Alexe M (2007) Phys Rev B 75:224113
34. Damjanovic D (1998) Rep Prog Phys 61:1267
35. Taylor DV, Damjanovic D (1998) Appl Phys Lett 73:2045
36. Gharb NB, Mckinstry ST (2005) J Appl Phys 97:064106
37. Hu SH, Hu GJ, Meng XJ, Wang GS, Sun JL, Guo SL, Chu JH, Dai N (2004) J Cryst Growth 260:109
38. Suzuki K, Kijima K (2005) Jpn J Appl Phys 44:8528
39. Wang Y, Ren X, Liu J, Zhang Z, Van F, Lu C, Zhu J, Shen H (1999) Ferroelectrics 231:1
40. Yan F, Bao P, Chan LW, Choy CL, Wang Y (2002) Thin Solid Films 406:282
41. Arlt G, Hennings D, With GD (1985) J Appl Phys 58:1619